

Time-aware Motion Planning in Dynamic Environments with Conformal Prediction

Kaier Liang¹

KAL221@LEHIGH.EDU

Licheng Luo²

LICHENGL@UCR.EDU

Yixuan Wang²

YWANG1457@UCR.EDU

Mingyu Cai²

MINGYU.CAI@UCR.EDU

Cristian Ioan Vasile¹

CVASILE@LEHIGH.EDU

¹*Mechanical Engineering and Mechanics Department, Lehigh University, PA, USA*

²*Department of Mechanical Engineering, University of California Riverside, CA, USA*

Abstract

Safe navigation in dynamic environments remains challenging due to uncertain obstacle behaviors and the lack of formal prediction guarantees. We propose two motion planning frameworks that leverage conformal prediction (CP): a global planner that integrates Safe Interval Path Planning (SIPP) for uncertainty-aware trajectory generation, and a local planner that performs online reactive planning. The global planner offers distribution-free safety guarantees for long-horizon navigation, while the local planner mitigates inaccuracies in obstacle trajectory predictions through adaptive CP, enabling robust and responsive motion in dynamic environments. To further enhance trajectory feasibility, we introduce an adaptive quantile mechanism in the CP-based uncertainty quantification. Instead of using a fixed confidence level, the quantile is automatically tuned to the optimal value that preserves trajectory feasibility, allowing the planner to adaptively tighten safety margins in regions with higher uncertainty. We validate the proposed framework through numerical experiments conducted in dynamic and cluttered environments. The project page is available at <https://time-aware-planning.github.io>

Keywords: Conformal Prediction, Motion Planning, Trajectory Prediction, Uncertainty Quantification, Machine Learning

1. Introduction

Robust navigation in dynamic environments remains a central challenge for autonomous agents Mavrogiannis et al. (2023); Rudenko et al. (2020). Applications such as mobile robots navigating crowded areas or drones operating in shared airspace require planners that can efficiently compute collision-free trajectories despite the uncertainty in predicting the motion of surrounding obstacles. Classical approaches to motion planning, such as dynamic window search or sampling-based planners Aoude et al. (2013), either neglect prediction uncertainty or rely on strong parametric assumptions about obstacle dynamics, resulting in overly conservative behavior or unsafe plans Phillips and Likhachev (2011). To handle such uncertainty, a variety of robust planning techniques have been developed. Chance-constrained motion planning Blackmore et al. (2011); Du Toit and Burdick (2011) incorporates stochastic bounds on obstacle trajectories, ensuring constraint satisfaction with high probability. Distributionally robust formulations extend this idea by optimizing against worst-case distributions within ambiguity sets—recent robotics examples include Wasserstein-robust risk maps and motion/control schemes Hakobyan and Yang (2021). Tube-based MPC contains deviations within tightened constraint sets and provides robust feasibility under bounded disturbances Zhang et al. (2022); Mayne et al. (2011). Reference governor-based methods (Garone et al., 2017; Liang et al.,

2024) address constraint satisfaction in complex systems by computing safety margins and navigation fields that guide the system toward feasible operating regions. Risk-sensitive /Conditional Value at Risk (CVaR)-based planners explicitly trade expected cost against tail risk (Chow et al., 2015). These methods provide theoretical safety guarantee but typically require strong assumptions on the underlying noise model (e.g., Gaussian errors, convex uncertainty sets) and often scale poorly in high-dimensional or long-horizon planning tasks. Modern online control approaches leverage Control Barrier Functions (CBFs) (Ames et al., 2019; Lopez et al., 2020) to ensure safety under uncertainty, incorporating robust and adaptive techniques to compensate for noisy observations and disturbance.

Recent advances in trajectory prediction using deep learning models provide high-quality forecasts of dynamic agents, but they lack calibrated measures of uncertainty. As a result, plans based directly on such predictions risk unsafe outcomes when the predictions deviate from reality. Conformal prediction (CP) has emerged as a powerful framework for providing distribution-free uncertainty quantification with finite-sample guarantees (Vovk et al., 2005; Sun et al., 2023; Strawn et al., 2023; Chee et al., 2024; Liang et al., 2025). By producing valid prediction regions around obstacle trajectories at a user-specified confidence level, CP enables principled reasoning about probabilistic guarantee. It has been applied to probabilistic verification tasks such as large language model validation (Wang et al., 2024; Cherian et al., 2024), temporal logic verification (Yu et al., 2026), semantic segmentation (Mossina et al., 2024) and so on. Lindemann et al. demonstrated how CP can be integrated into a model predictive control (MPC) framework to provide probabilistic safety guarantee in continuous state spaces (Lindemann et al., 2023). While this represents an important step forward, MPC-based formulations can be computationally expensive for long horizons, and their continuous nature makes them less suited for discrete, graph-based planning domains such as navigation on road networks, grids, or task-specific graphs. While split conformal prediction guarantee finite sample coverage under exchangeability, real deployments rarely preserve exchangeability between historical calibration data and the incoming stream. Recent adaptive conformal prediction(ACP) methods address this gap by coupling an online exchangeability diagnostic with a feedback-driven update that steers realized miscoverage to a target level without assuming exchangeability. (Dixit et al., 2022; Gibbs and Candès, 2021; Gibbs and Candès, 2024)

In this work, we integrate conformal prediction into Safe Interval Path Planning (SIPP) (Phillips and Likhachev, 2011) and extend it to a sampling-based framework for continuous domains. Our approach augments SIPP with confidence levels derived from conformal prediction, enabling the planner to reason about probabilistic safety alongside travel time. To handle continuous environments where online sensor feedback is available, we further develop a time-aware Adaptive Conformal Prediction Rapidly-Exploring Random Tree (ACP-RRT) algorithm that leverages real-time observations at each step to adaptively calibrate safety bounds, enabling local reactive planning while maintaining distribution-free safety guarantee. Together, these frameworks demonstrate how conformal prediction can provide unified, uncertainty-aware motion planning across both discrete and continuous settings—with Conformal Prediction Safe Interval Path Planning (CP-SIPP) suited for global, long-horizon planning and ACP-RRT designed for local, reactive navigation in response to incoming sensor data.

The main contributions of this paper are: (i) We introduce a CP-SIPP framework that integrates conformal prediction for global, long-horizon navigation with formal, distribution-free safety guarantee in discrete spatial-temporal domains. (ii) We propose optimization methods that balance trajectory feasibility, optimal cost, and CP confidence. (iii) We extend the conformal safety principle to continuous domains through a time-aware ACP-RRT that performs local, reactive planning by adaptively calibrating uncertainty bounds using online sensor feedback at each step, enabling probabilistically safe motion planning under distribution shift.

2. Preliminaries and Problem Formulation

2.1. Confidence Prediction for Dynamic Obstacles

Consider a controllable robot operating on a finite, undirected graph $G = (V, E)$, where $V \subset \mathbb{Z}^2$ represents discrete spatial locations and $E \subseteq V \times V$ encodes valid transitions between them. The agent's trajectory over a time horizon T is a sequence of vertices $\pi = (v_0, v_1, \dots, v_k)$, where $v_t \in V$ and $k \leq T$. The environment contains n dynamic obstacles $\mathcal{O} = \{\tau_1, \tau_2, \dots, \tau_n\}$, where each obstacle follows a continuous trajectory $\tau_i : [0, T] \rightarrow \mathbb{R}^2$ specifying its position over time. The true obstacle trajectories $\tau_i(t)$ are unknown and must be estimated from sensor data and motion models, yielding predicted trajectories $\hat{\tau}_i(t)$.

Since the predictions $\hat{\tau}_i(t)$ inevitably deviate from the true future positions, we employ *conformal prediction* (Lei et al., 2017), a statistical framework for constructing prediction regions with finite-sample, distribution-free guarantees. CP requires only the assumption of *exchangeability* between calibration and test data, rather than any specific parametric form, making it particularly suitable for real-world settings with uncertain or nonstationary dynamics. The key mechanism of CP is the *nonconformity score*, which quantifies the discrepancy between model predictions and ground truth. We define the nonconformity score at time t as the maximum prediction error across all obstacles, $R(t) = \max_{i=1, \dots, n} \|\hat{\tau}_i(t) - \tau_i(t)\|$ (Lindemann et al., 2023).

Given a calibration dataset \mathcal{D}_{cal} of historical obstacle trajectories, the conformal framework assumes that calibration and deployment data are exchangeable. When this assumption does not hold (e.g., under time-varying dynamics), a *weighted conformal prediction* approach (Barber et al., 2023) can be applied. The prediction threshold C_t is then chosen as the $(1 - \alpha)$ -quantile of the empirical distribution of calibration nonconformity scores, $C_t = \text{Quantile}_{1-\alpha}\{R_j(t) : j \in \mathcal{D}_{\text{cal}}\}$, where $\alpha \in [0, 1]$ is the user-specified miscoverage rate. This construction ensures that $P(R(t) \leq C_t) \geq 1 - \alpha$, providing a finite-sample coverage guarantee that holds under exchangeability without requiring any distributional assumptions on obstacle motion.

To integrate conformal prediction into discrete motion planning, we derive spatially indexed confidence values. For each grid location $s \in V$ and time t , we compute its distance to each predicted obstacle position as $d_i(s, t) = \|s - \hat{\tau}_i(t)\|$. The confidence that location s is safe at time t is then given by $c(s, t) = \frac{|\{j \in \mathcal{D}_{\text{cal}} : R_j(t) \leq \min_i d_i(s, t)\}|}{|\mathcal{D}_{\text{cal}}|}$. Here, $R_j(t)$ denotes the nonconformity score computed from the j -th calibration trajectory. Intuitively, $c(s, t)$ represents the empirical fraction of calibration samples whose maximum prediction error does not exceed the minimum safety margin $\min_i d_i(s, t)$. By the conformal prediction guarantee, if $c(s, t) \geq 1 - \alpha$, then location s is collision-free at time t with probability at least $1 - \alpha$ under exchangeability. This formulation yields distribution-free, finite-sample safety guarantees that hold regardless of the underlying obstacle motion distribution and allows the planner to trade off safety and performance by selecting appropriate confidence thresholds for each waypoint—higher confidence levels correspond to larger safety margins around predicted obstacle positions.

2.2. Problem Formulation

In dynamic environments with uncertain obstacle motion, a valid plan must ensure not only spatiotemporal feasibility but also probabilistic safety. Classical shortest-path formulations minimize travel time while enforcing connectivity, yet they cannot explicitly account for uncertainty induced by prediction errors. To bridge this gap, we introduce two complementary formulations: a global planning problem that employs pre-calibrated conformal thresholds for long-horizon navigation, and a local reactive planning problem that adapts safety margins online using sensor feedback. For

global planning in the absence of real-time observations, the objective is to compute a trajectory from start to goal that is both time-efficient and provably safe with respect to prediction uncertainty.

Problem 1 (Global Time-aware Motion Planning) *Given a start location v_{start} , a goal location v_{goal} , a time horizon T , a minimum confidence threshold $c_{min} \in [0, 1]$, and predicted obstacle trajectories $\{\hat{\tau}_i(t)\}_{i=1}^n$ with fixed calibration dataset, find an optimal trajectory π offline that solves:*

$$\min_{\pi} \sum_{j=0}^{k-1} (\gamma w(v_j, v_{j+1}) + (1 - \gamma)c_j) \quad (1a)$$

$$\text{subject to } v_0 = v_{start}, \quad v_k = v_{goal} \quad (\exists k \leq T) \quad (1b)$$

$$(v_j, v_{j+1}) \in E, \quad v_j \in \mathcal{S}(c_j, t_j), \quad \forall j \in \{0, \dots, k\} \quad (1c)$$

where $\gamma \in [0, 1]$ balances travel time and safety, $w(v_j, v_{j+1})$ is the edge cost e.g., travel time, and $\mathcal{S}(c_j, t_j) = \{s \in V : c(s, t_j) \geq c_j\}$ is the conformal safe set at time t_j .

Problem 2 (Local Reactive Time-aware Motion Planning) *Given current state $(v_{current}, t_{current})$, goal region v_{goal} , sensor horizon H_{local} , predicted obstacle trajectories $\{\hat{\tau}_i(t)\}_{i=1}^n$, find a feasible trajectory online $\pi_{local} : [t_{current}, t_{current} + H_{local}] \rightarrow \mathcal{X}$ that starts at $v_{current}$, maintain conformal safety confidence $C_t(c(t))$ from obstacles, and makes progress toward v_{goal} .*

The key difference is that Problem 1 aims to compute an optimal long-horizon path offline using a fixed calibration dataset, whereas Problem 2 focuses on finding a feasible path online that is calibration dataset free and adapts to distribution shifts detected through real-time feedback.

3. Solution

We present two planning frameworks that address uncertainty in dynamic environments through conformal prediction. The first framework (Section 3.1) solves Problem 1 for global, long-horizon planning using pre-calibrated conformal dataset. We develop two algorithmic approaches: a space-time planning formulation with explicit confidence enumeration, and a computationally efficient Safe Interval Path Planning (SIPP) extension that compresses temporal information while maintaining probabilistic safety guarantees. The second framework (Section 3.2) solves Problem 2 for local reactive planning with online observations, where we develop a sampling-based approach that adaptively calibrates safety bounds in response to distribution shift.

3.1. Global Time-Aware Planning

3.1.1. Space-time Planning with Confidence: In traditional space-time planning, the dynamic environment is modeled as a graph where states $s = (v, t)$ explicitly combine spatial locations $v \in V$ with discrete time steps $t \in \{0, 1, \dots, T\}$. This formulation produces a state space of size $O(|V| \times T)$ by enumerating all spatial-temporal configurations. While this approach requires exploring a large state space, it guarantees finding the globally optimal solution to Problem 1.

To integrate conformal prediction with space-time planning, we augment the space-time representation to include confidence levels: $\hat{s} = (v, c, t)$, where $v \in V$ is the spatial vertex, $c \in \mathcal{C}$ is the discrete confidence level from our finite confidence set $\mathcal{C} = \{c_1, c_2, \dots, c_m\}$, and $t \in \{0, 1, \dots, T\}$ is the time step. We construct a confidence space-time graph $G_{st} = (V_{st}, E_{st})$ where:

- $V_{st} = \{(v, c, t) : v \in V, t \in \{0, \dots, T\}, c \in \mathcal{C}, c(v, t) \geq c_{min}\}$ where for each state, c represents the discrete confidence level assigned based on the empirical confidence $c(v, t)$.

- $E_{st} = \{((v, c, t), (v', c', t')) : (v, v') \in E, t' = t + w(v, v'), c' \text{ is the confidence level at } (v', t')\}$.

Given the confidence space-time graph G_{ST} , we find optimal paths using standard graph search algorithms such as A*. Edge weights combine travel time and safety:

$$w((v, c, t), (v', c', t')) = (1 - \gamma) \cdot w(v, v') - \gamma \cdot \log(c') \quad (2)$$

where $\gamma \in [0, 1]$ controls the trade-off as in (1a): $\gamma = 0$ yields purely time-optimal paths, $\gamma = 1$ maximizes confidence, and intermediate values balance both objectives. When $\gamma = 0$ and multiple paths achieve equal travel time, ties are broken by preferring higher-confidence states.

The key advantage of this approach is its completeness: the explicit enumeration of all spatial-temporal-confidence combinations guarantees finding the globally optimal solution. However, this comes at the cost of a state space that grows as $O(|V| \times T)$, which becomes prohibitive for long planning horizons. This motivates our confidence-augmented SIPP approach in the next section, which achieves similar optimality guarantees with dramatically reduced computational complexity.

3.1.2. CP-Augmented SIPP: While the space–time formulation can achieve globally optimal solutions by explicitly enumerating all spatiotemporal states, it becomes computationally prohibitive as planning horizons or environmental complexity increase. The number of discrete time steps grows rapidly, leading to an explosion in state–time combinations and making direct search intractable for large-scale problems. Safe Interval Path Planning (Phillips and Likhachev, 2011) mitigates this issue by recognizing that, although time is continuous, the number of *contiguous safe intervals* at each location is typically much smaller than the total number of timesteps. Instead of maintaining one state per time step, SIPP aggregates all collision-free times at a vertex into maximal intervals, thereby compressing temporal information without sacrificing optimality with respect to arrival time. In the standard SIPP formulation, each spatial vertex $v \in V$ maintains a timeline of alternating safe and unsafe intervals. A safe interval $I = [t_a, t_b)$ denotes one maximal contiguous period during which vertex v is guaranteed to be collision-free.

Each state is represented as $s = (v, I)$, indicating that the agent is at vertex v during interval I . Thus, a single vertex may correspond to multiple non-overlapping safe intervals, each forming a distinct state. This representation dramatically reduces the number of states compared with the full space–time grid. During search, SIPP stores for each state s the earliest feasible arrival time $g(s) \in [t_a, t_b]$, which serves as the accumulated cost (i.e., the g -value in A*). The heuristic $h(s)$ estimates the remaining travel time to the goal (e.g., Euclidean distance divided by maximum speed), and the evaluation function is $f(s) = g(s) + h(s)$.

When expanding a state, SIPP determines the earliest departure time within I that allows collision-free arrival at a successor state. This on-the-fly computation of feasible transitions based on arrival time is what enables SIPP’s temporal compression and efficiency. To incorporate probabilistic safety guarantees, we extend SIPP by discrete confidence levels $\mathcal{C} = \{c^1, c^2, \dots, c^m\}$ in decreasing order, where each $c^i \in [0, 1]$ represents a required confidence threshold. A confidence-augmented state is defined as $\hat{s} = (v, c, I)$, where $v \in V$ is a spatial vertex, $c \in \mathcal{C}$ is the confidence level, and $I = [t_a, t_b)$ is the safe interval corresponding to that confidence. For each vertex–confidence pair (v, c) , we compute the corresponding safe time intervals where vertex v remains collision-free at level c : $\min_{i \in \{1, \dots, n\}} \|v - \tau_i(t)\| > Q_{1-\alpha}^c(t), \quad \forall t \in [t_a, t_b)$, where $Q_{1-\alpha}^c(t)$ is the $(1 - \alpha)$ -quantile of the prediction error from the conformal prediction model. In practice, safe intervals are obtained by discretizing time and identifying the maximal contiguous segments satisfying the above condition.

The search cost is defined in terms of time, $\hat{g}(\hat{s}) = t_{\text{arrival}}$, where t_{arrival} denotes the arrival time at state \hat{s} . The heuristic function is given by $\hat{h}(\hat{s}) = h(v, v_{\text{goal}})$, representing the estimated remaining travel time from vertex v to the goal vertex v_{goal} . When multiple states share the same f -score, the algorithm prioritizes those with higher confidence levels, thereby biasing the search toward safer

trajectories without sacrificing time optimality. If both the f -scores and confidence levels are identical, ties are resolved arbitrarily. Each state transition $(v_j, c_j, I_j, t_j) \rightarrow (v_{j+1}, c_{j+1}, I_{j+1}, t_{j+1})$ must satisfy: (i). spatial connectivity: $(v_j, v_{j+1}) \in E$; (ii). temporal feasibility: $t_{j+1} = t_j + w(v_j, v_{j+1})$, where $w(\cdot)$ denotes the travel time; (iii). departure constraint: $t_j \leq t_{\text{end}}^{I_j}$; and (iv) arrival constraint: $t_{\text{start}}^{I_{j+1}} \leq t_{j+1} \leq t_{\text{end}}^{I_{j+1}}$. The confidence level c_{j+1} is selected from any admissible value at vertex v_{j+1} satisfying $c_{j+1} \geq c_{\min}$. Successor states below this threshold are pruned to improve efficiency.

Theorem 1 (Trajectory-Level Safety under Marginal Conformal Guarantees) *Let π be any trajectory with collision-check grid $\mathcal{T}(\pi) = \{t_0, \dots, t_k\}$ generated by a planner employing conformal prediction. For each $t \in \mathcal{T}(\pi)$, let E_t denote the event that the robot's configuration at time t lies within the conformal safety set \mathcal{S}_t^c constructed at confidence level $c_t \in [0, 1]$. Assume that the per-time coverage guarantees hold marginally, that is, $\Pr(E_t) \geq c_t$ for all $t \in \mathcal{T}(\pi)$.*

Then, the probability that the trajectory remains safe at all times satisfies $\Pr\left(\bigcap_{t \in \mathcal{T}(\pi)} E_t\right) \geq 1 - \sum_{t \in \mathcal{T}(\pi)} (1 - c_t)$. Equivalently, the probability of a collision or safety violation along the trajectory satisfies $\Pr\left(\bigcup_{t \in \mathcal{T}(\pi)} E_t^C\right) \leq \sum_{t \in \mathcal{T}(\pi)} (1 - c_t)$, where E_t^C denotes the complement of E_t . In particular, if the confidence level is uniform, $c_t \equiv 1 - \alpha$, then $\Pr\left(\bigcup_{t \in \mathcal{T}(\pi)} E_t^C\right) \leq k\alpha$.

Proof Let E_t be the per-time safety events with marginal coverage $\Pr(E_t) \geq c_t$. By the complement identity, $\Pr\left(\bigcap_{t \in \mathcal{T}(\pi)} E_t\right) = 1 - \Pr\left(\bigcup_{t \in \mathcal{T}(\pi)} E_t^C\right)$. Boole's inequality state that $\Pr(\cup_t A_t) \leq \sum_t \Pr(A_t)$ for any events $\{A_t\}$ (Grimmett and Stirzaker, 2001). Applying it with $A_t = E_t^C$ and using $\Pr(E_t^C) = 1 - \Pr(E_t) \leq 1 - c_t$ yields $\Pr\left(\bigcup_{t \in \mathcal{T}(\pi)} E_t^C\right) \leq \sum_{t \in \mathcal{T}(\pi)} (1 - c_t)$ hence $\Pr\left(\bigcap_{t \in \mathcal{T}(\pi)} E_t\right) \geq 1 - \sum_{t \in \mathcal{T}(\pi)} (1 - c_t)$. In the uniform case $c_t \equiv 1 - \alpha$, this reduces to $\Pr\left(\bigcup_{t \in \mathcal{T}(\pi)} E_t^C\right) \leq k\alpha$ with $k = |\mathcal{T}(\pi)|$.

3.2. Local Reactive Planning with Adaptive Conformal Prediction

While the confidence-augmented SIPP formulation provides a principled and complete solution for time-aware motion planning on discretized state spaces, its reliance on a pre-defined graph and enumerated safe intervals limits scalability in high-dimensional or continuous domains. To address this, we extend the same conformal-safety framework to a sampling-based setting, where the planner incrementally explores the continuous space–time manifold using random sampling rather than explicit graph expansion. In this regime, the safety of each candidate motion is evaluated through adaptive conformal prediction (ACP), which supplies calibrated uncertainty bounds on obstacle trajectories for a time-varying confidence schedule. This yields a time-aware conformal RRT (ACP-RRT) that preserves the probabilistic safety guarantees of the SIPP formulation while offering the flexibility and scalability of sampling-based planning.

3.2.1. CALIBRATION-FREE ADAPTIVE CONFORMAL PREDICTION

Exchangeability Diagnostics: Real deployments rarely preserve exchangeability between the historical calibration dataset and the incoming prediction-observation stream. Before passing confidence to SIPP, we therefore insert an exchangeability gate. Let $\mathcal{D}_{\text{cal}} = \{R_j\}_{j=1}^n$ be the calibration scores defined in §2.1. As soon as feedback becomes available online, we collect a warm-up batch of new scores $\mathcal{D}_{\text{new}} = \{R_t\}_{t=t_0}^{t_0+W_0-1}$. We assess whether the marginal score distribution remains unchange across the \mathcal{D}_{cal} and \mathcal{D}_{new} . The equality condition is $\mathcal{L}(R | \text{cal}) = \mathcal{L}(R | \text{new})$.

Deviation from this criterion is quantified by the two-sample Kolmogorov–Smirnov (KS) distance $D = \sup_{x \in \mathbb{R}} |\hat{F}_{\text{cal}}(x) - \hat{F}_{\text{new}}(x)|$, where \hat{F}_{cal} and \hat{F}_{new} are the empirical CDFs of \mathcal{D}_{cal} and \mathcal{D}_{new} . To maintain the nominal level under short-range serial dependence, we approximate the null distribution of D using a time-robust permutation: pool $Z = (\mathcal{D}_{\text{cal}} \| \mathcal{D}_{\text{new}})$, split Z into contiguous blocks of length B , randomly permute the blocks to obtain Z^* , and resplit Z^* into $(\mathcal{D}_{\text{cal}}^*, \mathcal{D}_{\text{new}}^*)$. The permuted statistic is

$$D^* = \sup_{x \in \mathbb{R}} |\hat{F}_{\text{cal}}^*(x) - \hat{F}_{\text{new}}^*(x)| \quad (3)$$

Repeating this procedure N times yields $\{D^{*(b)}\}_{b=1}^N$ and the unbiased permutation p-value

$$p = \frac{1 + \sum_{b=1}^N \mathbf{1}\{D^{*(b)} \geq D\}}{N+1} \quad (4)$$

if $p < \alpha_{\text{gate}}$, the gate rejects and ACP is activated.

Adaptive update rule When the exchangeability test rejects, we discontinue the use of calibration quantiles and switch to calibration-free ACP. Let R_t be the nonconformity score at time t . We introduce a positive scale λ_t and a fixed monotone threshold map $C(\lambda)$.

$$H(\lambda_t) = \lambda_t d_{\min}(s_t), \quad d_{\min}(s_t) = \min_i \inf_{\tau \in I(s_t)} \|v(s_t) - \hat{r}_i(\tau)\| \quad (5)$$

where s_t is the current vertex-time state, $I(s_t)$ is its SIPP safe interval, $v(s_t)$ is the spatial location at s_t , and $\hat{r}_i(\cdot)$ denotes the predicted trajectory of obstacle i . Define the miscoverage indicator

$$e_t = \mathbf{1}\{R_t > H_t(\lambda_t)\} \in \{0, 1\} \quad (6)$$

During deployment the map $H(\cdot)$ remains fixed; only the positive scale λ_t adapts online, we update

$$\lambda_{t+1} = \Pi_{[\lambda_{\min}, \lambda_{\max}]}(\lambda_t \exp\{\kappa(e_t - \alpha)\}) \quad (7)$$

initialized at $\lambda_0 = 1$. Under miscoverage ($e_t = 1$) increases λ_t so that the next region is more conservative; under coverage ($e_t = 0$) it decreases.

Regularity We assume that the miscoverage response $p(\lambda) = \mathbb{E}[e_t \mid \lambda_t = \lambda, \mathcal{F}_{t-1}]$ is strictly decreasing in λ on a compact interval $[\lambda_{\min}, \lambda_{\max}]$ that brackets the target, $p(\lambda_{\min}) > \alpha$ and $p(\lambda_{\max}) < \alpha$. Feedback exhibits short-range dependence so that time averages stabilize. Under these standard conditions and a small constant step size, the one-dimensional feedback on λ_t yields the time-average tracking guarantee state below.

Theorem 2 (Time-average coverage control for calibration-free ACP) *Under the regularity above and a constant step size $\kappa > 0$, the closed loop remains in $[\lambda_{\min}, \lambda_{\max}]$ and the realized miscoverage frequency satisfies*

$$\left| \frac{1}{T} \sum_{t=1}^T e_t - \alpha \right| = \mathcal{O}_{\mathbb{P}}(\kappa) + \mathcal{O}_{\mathbb{P}}(T^{-1/2})$$

Therefore a sufficiently small κ keeps the time-average miscoverage in an \mathcal{O}_{κ} band around α without assuming exchangeability with the historical data.

Proof: Let $z_t = \log \lambda_t$, so the multiplicative update becomes the projected additive recursion $z_{t+1} = \Pi_{[\log \lambda_{\min}, \log \lambda_{\max}]}(z_t + \kappa(e_t - \alpha))$. Write $e_t = p(\lambda_t) + \xi_t$, $\{\xi_t\}$ is bounded martingale difference under the same weak dependence used by the gate. Let $z^* = \log \lambda^*$ with $p(\lambda^*) = \alpha$, and set $V_t = (z_t - z^*)^2$. By strict monotonicity of p in the compact interval $[\lambda_{\min}, \lambda_{\max}]$, for every $\varepsilon > 0$ there exists $\rho(\varepsilon) > 0$ such that whenever $|z_t - z^*| \geq \varepsilon$ one has $(z_t - z^*)(p(\lambda_t) - \alpha) \leq -\rho(\varepsilon)(z_t - z^*)^2$. Using projection nonexpansiveness, $\mathbb{E}[V_{t+1} - V_t | \mathcal{F}_{t-1}] \leq -2\kappa\rho(\varepsilon)V_t + \kappa^2$. Summing yields $\frac{1}{T} \sum_{t=1}^T \mathbb{E}[V_t] = O(\kappa)$. Averaging $e_t - \alpha = \{p(\lambda_t) - \alpha\} + \xi_t$ gives $\left| \frac{1}{T} \sum_{t=1}^T (e_t - \alpha) \right| = O(\kappa) + \mathcal{O}_{\mathbb{P}}(T^{-1/2})$. Since $\frac{1}{T} \sum \xi_t = \mathcal{O}_{\mathbb{P}}(T^{-1/2})$. With diminishing step sizes satisfying $\sum_t \kappa_t = \infty$ and $\sum_t \kappa_t^2 < \infty$, the bias vanishes and $\frac{1}{T} \sum_{t=1}^T e_t \xrightarrow{\mathbb{P}} \alpha$.

3.2.2. TIME-AWARE CONFORMAL RRT

The time-aware conformal RRT extends space-time RRT approaches ([Grothe et al., 2022](#); [Sintov and Shapiro, 2014](#)), which represent nodes as (x, t) pairs, by augmenting each node with a confidence level c to explicitly reason about prediction uncertainty through conformal prediction. When expanding the tree, the algorithm samples a random spatial state, connects it to the nearest node, and assigns an arrival time based on the travel distance and robot speed. Along each edge, the planner predicts the robot's motion forward in time and checks for collisions against predicted obstacle trajectories. At each intermediate step, the confidence level $c(t)$ is obtained from a predefined decay schedule, and ACP provides the corresponding prediction radius for that horizon. The edge is accepted only if all sampled points along it remain outside the ACP-inflated obstacle regions, ensuring time-consistent conformal safety.

To avoid the problem being infeasible due to a long prediction horizon and to capture the increasing uncertainty of long-term forecasts, the planner employs a time-varying confidence schedule $c(t)$ that smoothly decays from an initial high confidence $c_{\text{start}} \in \mathcal{C}$ to a lower terminal confidence $c_{\text{end}} \in \mathcal{C}$ over the planning horizon H :

$$c(t) = c_{\text{end}} + (c_{\text{start}} - c_{\text{end}}) \left(1 - \frac{t}{H}\right). \quad (8)$$

This schedule reflects the intuition that near-term predictions are more reliable and should be treated conservatively, while distant predictions can tolerate greater uncertainty. As summarized in Algorithm 1, the planner grows the conformal RRT in a receding-horizon manner: at each planning cycle, it constructs a time-aware tree using the current ACP calibration based on prediction step and requiring confidence, executes only the first motion segment (RRT node), and then incorporates new observations to update the ACP bounds. This closed-loop procedure continuously adapts both the uncertainty estimates and the effective confidence level over time.

4. Results

We evaluate our two planning frameworks through simulation experiments. Section 4.1 presents results for CP-SIPP, demonstrating global planning performance on grid environments with dynamic obstacles. Section 4.2 evaluates ACP-RRT for local reactive planning in continuous domains, showing how adaptive conformal prediction maintains safety under distribution shift. We analyze path quality, and safety guarantees for both approaches.

Algorithm 1 ACP-RRT

Input: Start node (x_s, t_s, c_s) , goal region $\mathcal{X}_{\text{goal}}$, ACP model \mathcal{A}

Output: Probabilistically safe path to $\mathcal{X}_{\text{goal}}$

```

1  $\mathcal{T} \leftarrow \{(x_s, t_s, c_s)\}$ 
2 while goal not reached do
3   Sample  $x_{\text{rand}} \in \mathcal{X}$   $(x_{\text{near}}, t_{\text{near}}, c_{\text{near}}) \leftarrow \text{Nearest}(\mathcal{T}, x_{\text{rand}})$ 
    $x_{\text{new}} \leftarrow \text{Steer}(x_{\text{near}}, x_{\text{rand}})$ 
    $t_{\text{new}} \leftarrow t_{\text{near}} + \frac{\|x_{\text{new}} - x_{\text{near}}\|}{v_{\max}}$ 
    $c_{\text{new}} \leftarrow c(t_{\text{new}})$  from (8);
   if  $|x_{\text{new}} - \tau_i| > ACP(t_{\text{new}}, c_{\text{new}})$  for all  $i$  then
4     Add  $(x_{\text{new}}, t_{\text{new}}, c_{\text{new}})$  to  $\mathcal{T}$  if  $x_{\text{new}} \in \mathcal{X}_{\text{goal}}$  then
5       return Path( $\mathcal{T}$ )
6 return failure

```

4.1. CP-SIPP

To further illustrate how uncertainty evolves across prediction horizons and confidence levels, we visualize the quantile table generated by the Seq2Seq LSTM-based motion prediction model (Sutskever et al., 2014). As shown in Fig. 1, CP-SIPP demonstrates its ability to perform uncertainty-aware navigation in complex environments with dynamic obstacles. By incorporating conformal prediction into the SIPP framework, the planner adaptively adjusts its trajectory to avoid predicted obstacle regions while maintaining computational efficiency. The green line indicates the executed path, dark red dots represent predicted obstacle centers, and light red disks denote their 95% quantile conformal prediction confidence regions rendered at the current timestep.

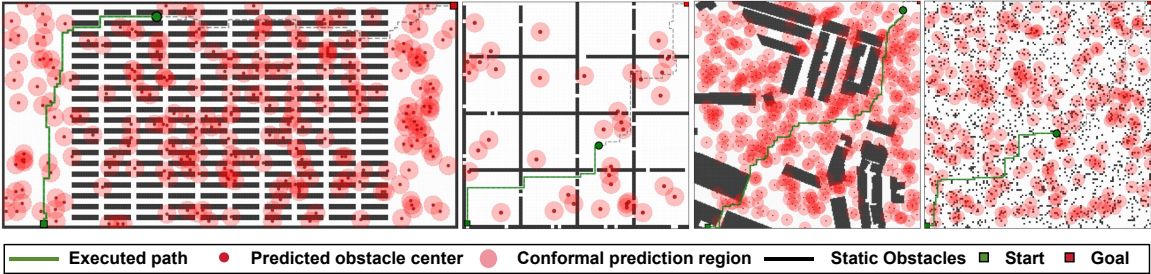


Figure 1: CP-SIPP: four frames showing uncertainty-aware CP-SIPP navigating through complex environments with dynamic obstacles

4.2. ACP-RRT

Fig. 3 illustrates the performance of the proposed ACP-RRT with a planning horizon of $H = 50$. We introduce three dynamic obstacles, and ACP is employed to generate confidence regions for their predicted trajectories at each time step. The figure presents snapshots of the planning process at $t = 0$, $t = 25$, and $t = 45$. As the prediction horizon increases, the RRT accepts nodes with lower confidence levels, allowing it to maintain feasibility while adapting to the growing trajectory prediction uncertainty.

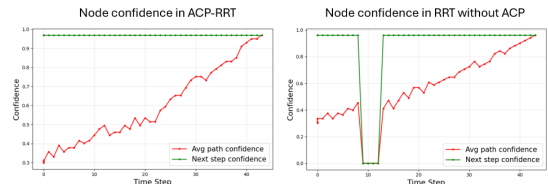


Figure 2: Confidence Evolution Comparison: left: The ACP-RRT planner successfully maintains high confidence. right: The baseline RRT (without ACP) fails with a collision at $t = [9, 12]$.

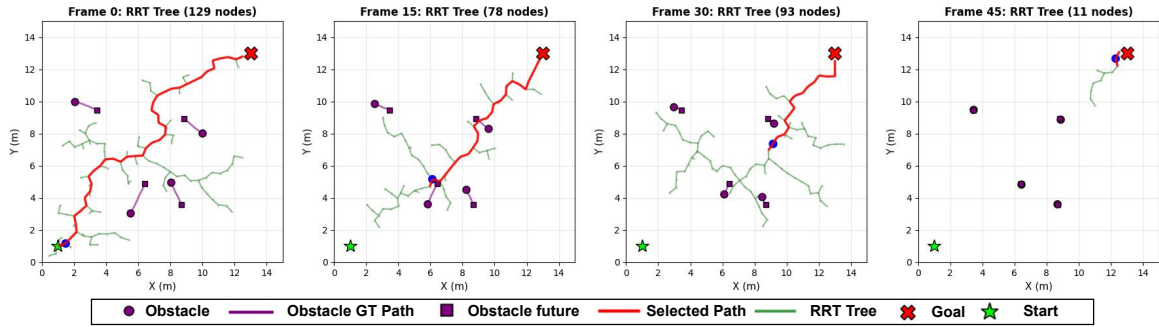


Figure 3: ACP-RRT: three frames showing online ACP-RRT adaptive generating trees to navigating through obstacles with uncertainty

Fig. 2 (left) illustrates the evolution of the average node confidence during planning. As time progresses, the agent requires fewer steps to reach the target, resulting in shorter prediction horizons and consequently requiring fewer confidence regions. This leads to an overall increase in the average node confidence of the constructed RRT path over time. Meanwhile, due to the receding-horizon structure and the adaptive confidence update rule in (8), the confidence associated with the immediate next step consistently remains the highest throughout the planning process. In contrast, Fig. 2 (right) shows the baseline method implementing reactive RRT without ACP, where confidence is validated post-sampling rather than proactively incorporated during tree expansion. This approach fails with a collision at $t = [9, 12]$, where the confidence level drops to zero.

5. Conclusion

We presented two motion planning frameworks that integrate conformal prediction to enable uncertainty-aware navigation in dynamic environments. The first, CP-SIPP, extends the classical SIPP formulation by incorporating discrete confidence levels derived from conformal prediction, allowing the planner to compute time-optimal trajectories under formal, distribution-free probabilistic safety guarantees. The second, ACP-RRT, generalizes these principles to continuous domains through a sampling-based approach that adaptively adjusts safety bounds online. Together, these frameworks demonstrate how conformal prediction can provide a unified foundation for efficient, and provably safe motion planning under uncertainty.

References

- Aaron D Ames, Samuel Coogan, Magnus Egerstedt, Gennaro Notomista, Koushil Sreenath, and Paulo Tabuada. Control barrier functions: Theory and applications. In *2019 18th European control conference (ECC)*, pages 3420–3431. Ieee, 2019.
- Georges S Aoude, Brandon D Luders, Joshua M Joseph, Nicholas Roy, and Jonathan P How. Probabilistically safe motion planning to avoid dynamic obstacles with uncertain motion patterns. *Autonomous Robots*, 35(1):51–76, 2013.
- Rina Foygel Barber, Emmanuel J Candès, Aaditya Ramdas, and Ryan J Tibshirani. Conformal prediction beyond exchangeability. *The Annals of Statistics*, 51(2):816–845, 2023.
- Lars Blackmore, Masahiro Ono, and Brian C Williams. Chance-constrained optimal path planning with obstacles. *IEEE Transactions on Robotics*, 27(6):1080–1094, 2011.

Kong Yao Chee, Thales C Silva, M Ani Hsieh, and George J Pappas. Uncertainty quantification and robustification of model-based controllers using conformal prediction. In *6th Annual Learning for Dynamics & Control Conference*, pages 528–540. PMLR, 2024.

John Cherian, Isaac Gibbs, and Emmanuel Candès. Large language model validity via enhanced conformal prediction methods. *Advances in Neural Information Processing Systems*, 37:114812–114842, 2024.

Yinlam Chow, Aviv Tamar, Shie Mannor, and Marco Pavone. Risk-sensitive and robust decision-making: a cvar optimization approach. *Advances in neural information processing systems*, 28, 2015.

Anushri Dixit, Lars Lindemann, Skylar Wei, Matthew Cleaveland, George J. Pappas, and Joel W. Burdick. Adaptive conformal prediction for motion planning among dynamic agents, 2022.

Noel E Du Toit and Joel W Burdick. Robot motion planning in dynamic, uncertain environments. *IEEE Transactions on Robotics*, 28(1):101–115, 2011.

Emanuele Garone, Stefano Di Cairano, and Ilya Kolmanovsky. Reference and command governors for systems with constraints: A survey on theory and applications. *Automatica*, 75:306–328, 2017.

Isaac Gibbs and Emmanuel J. Candès. Conformal inference for online prediction with arbitrary distribution shifts. *Journal of Machine Learning Research*, 25(162):1–36, 2024.

Isaac Gibbs and Emmanuel Candès. Adaptive conformal inference under distribution shift, 2021.

Geoffrey R Grimmett and David R Stirzaker. *Probability and Random Processes*. Oxford University Press, 05 2001. ISBN 9780198572237. doi: 10.1093/oso/9780198572237.001.0001.

Francesco Grothe, Valentin N Hartmann, Andreas Orthey, and Marc Toussaint. St-rrt*: Asymptotically-optimal bidirectional motion planning through space-time. In *2022 International Conference on Robotics and Automation (ICRA)*, pages 3314–3320. IEEE, 2022.

Astghik Hakobyan and Insoon Yang. Wasserstein distributionally robust motion control for collision avoidance using conditional value-at-risk. *IEEE Transactions on Robotics*, 38(2):939–957, 2021.

Jing Lei, Max G’Sell, Alessandro Rinaldo, Ryan J. Tibshirani, and Larry Wasserman. Distribution-free predictive inference for regression, 2017.

Kaier Liang, Mingyu Cai, and Cristian-Ioan Vasile. Control barrier function for linearizable systems with high relative degrees from signal temporal logics: A reference governor approach. In *2024 American Control Conference (ACC)*, pages 1676–1681. IEEE, 2024.

Kaier Liang, Guang Yang, Mingyu Cai, and Cristian-Ioan Vasile. Safe navigation in dynamic environments using data-driven koopman operators and conformal prediction. *arXiv preprint arXiv:2504.00352*, 2025.

Lars Lindemann, Matthew Cleaveland, Gihyun Shim, and George J Pappas. Safe planning in dynamic environments using conformal prediction. *IEEE Robotics and Automation Letters*, 8(8):5116–5123, 2023.

Brett T Lopez, Jean-Jacques E Slotine, and Jonathan P How. Robust adaptive control barrier functions: An adaptive and data-driven approach to safety. *IEEE Control Systems Letters*, 5(3):1031–1036, 2020.

Christoforos Mavrogiannis, Francesca Baldini, Allan Wang, Dapeng Zhao, Pete Trautman, Aaron Steinfeld, and Jean Oh. Core challenges of social robot navigation: A survey. *ACM Transactions on Human-Robot Interaction*, 12(3):1–39, 2023.

David Q Mayne, Erric C Kerrigan, EJ Van Wyk, and Paola Falugi. Tube-based robust nonlinear model predictive control. *International journal of robust and nonlinear control*, 21(11):1341–1353, 2011.

Luca Mossina, Joseba Dalmau, and Léo Andéol. Conformal semantic image segmentation: Post-hoc quantification of predictive uncertainty. In *Proceedings of the IEEE/CVF Conference on Computer Vision and Pattern Recognition*, pages 3574–3584, 2024.

Mike Phillips and Maxim Likhachev. Sipp: Safe interval path planning for dynamic environments. In *2011 IEEE international conference on robotics and automation*, pages 5628–5635. IEEE, 2011.

Andrey Rudenko, Luigi Palmieri, Michael Herman, Kris M Kitani, Dariu M Gavrila, and Kai O Arras. Human motion trajectory prediction: A survey. *The International Journal of Robotics Research*, 39(8):895–935, 2020.

Avishai Sintov and Amir Shapiro. Time-based rrt algorithm for rendezvous planning of two dynamic systems. In *2014 IEEE International Conference on Robotics and Automation (ICRA)*, pages 6745–6750. IEEE, 2014.

Kegan J Strawn, Nora Ayanian, and Lars Lindemann. Conformal predictive safety filter for rl controllers in dynamic environments. *IEEE Robotics and Automation Letters*, 8(11):7833–7840, 2023.

Jiankai Sun, Yiqi Jiang, Jianing Qiu, Parth Nobel, Mykel J Kochenderfer, and Mac Schwager. Conformal prediction for uncertainty-aware planning with diffusion dynamics model. *Advances in Neural Information Processing Systems*, 36:80324–80337, 2023.

Ilya Sutskever, Oriol Vinyals, and Quoc V. Le. Sequence to sequence learning with neural networks, 2014. URL <https://arxiv.org/abs/1409.3215>.

Vladimir Vovk, Alexander Gammerman, and Glenn Shafer. *Algorithmic learning in a random world*. Springer, 2005.

Jun Wang, Jiaming Tong, Kaiyuan Tan, Yevgeniy Vorobeychik, and Yiannis Kantaros. Conformal temporal logic planning using large language models. *ACM Transactions on Cyber-Physical Systems*, 2024.

Xinyi Yu, Yiqi Zhao, Xiang Yin, and Lars Lindemann. Signal temporal logic control synthesis among uncontrollable dynamic agents with conformal prediction. *Automatica*, 183:112616, 2026.

Xinglong Zhang, Wei Pan, Riccardo Scattolini, Shuyou Yu, and Xin Xu. Robust tube-based model predictive control with koopman operators. *Automatica*, 137:110114, 2022.